



## High-pressure behavior of beta-Ga<sub>2</sub>O<sub>3</sub> nanocrystals

Wang, H.; He, Y.; Chen, W.; Zeng, Y.W.; Ståhl, Kenny; Kikegawa, T.; Jiang, J.Z.

*Published in:*  
Journal of Applied Physics

*Link to article, DOI:*  
[10.1063/1.3296121](https://doi.org/10.1063/1.3296121)

*Publication date:*  
2010

*Document Version*  
Publisher's PDF, also known as Version of record

[Link back to DTU Orbit](#)

*Citation (APA):*  
Wang, H., He, Y., Chen, W., Zeng, Y. W., Ståhl, K., Kikegawa, T., & Jiang, J. Z. (2010). High-pressure behavior of beta-Ga<sub>2</sub>O<sub>3</sub> nanocrystals. *Journal of Applied Physics*, 107(3), 033520. <https://doi.org/10.1063/1.3296121>

---

### General rights

Copyright and moral rights for the publications made accessible in the public portal are retained by the authors and/or other copyright owners and it is a condition of accessing publications that users recognise and abide by the legal requirements associated with these rights.

- Users may download and print one copy of any publication from the public portal for the purpose of private study or research.
- You may not further distribute the material or use it for any profit-making activity or commercial gain
- You may freely distribute the URL identifying the publication in the public portal

If you believe that this document breaches copyright please contact us providing details, and we will remove access to the work immediately and investigate your claim.

## High-pressure behavior of $\beta$ -Ga<sub>2</sub>O<sub>3</sub> nanocrystals

H. Wang,<sup>1</sup> Y. He,<sup>1</sup> W. Chen,<sup>1</sup> Y. W. Zeng,<sup>1,2</sup> K. Stahl,<sup>3</sup> T. Kikegawa,<sup>4</sup> and J. Z. Jiang<sup>1,a)</sup>

<sup>1</sup>International Center for New-Structured Materials (ICNSM) and Laboratory of New-Structured Materials, Department of Materials Science and Engineering, Zhejiang University, Hangzhou 310027, People's Republic of China

<sup>2</sup>Center of Analysis and Measurement, Zhejiang University, Hangzhou 310027, People's Republic of China

<sup>3</sup>Department of Chemistry, Technical University of Denmark, DK-2800 Lyngby, Denmark

<sup>4</sup>Photon Factory, Institute of Materials Structure Science, High Energy Accelerator Research Organization, 1-1 Oho, Tsukuba, Ibaraki 305-0801, Japan

(Received 8 October 2009; accepted 29 December 2009; published online 9 February 2010)

Freestanding nanocrystalline  $\beta$ -Ga<sub>2</sub>O<sub>3</sub> particles with an average grain size of 14 nm prepared by chemical method was investigated by angle-dispersive synchrotron x-ray diffraction in diamond-anvil cell up to 64.9 GPa at ambient temperature. The evolution of x-ray diffraction patterns indicated that nanocrystalline monoclinic  $\beta$ -Ga<sub>2</sub>O<sub>3</sub> underwent a phase transition to rhombohedral  $\alpha$ -Ga<sub>2</sub>O<sub>3</sub>. It was found that  $\beta$ - to  $\alpha$ -Ga<sub>2</sub>O<sub>3</sub> transition began at about 13.6–16.4 GPa, and extended up to 39.2 GPa. At the highest pressure used, only  $\alpha$ -Ga<sub>2</sub>O<sub>3</sub> was present, which remained after pressure release. A Birch–Murnaghan fit to the  $P$ - $V$  data yielded a zero-pressure bulk modulus at fixed  $B'_0=4$ :  $B_0=228(9)$  GPa and  $B_0=333(19)$  GPa for  $\beta$ -Ga<sub>2</sub>O<sub>3</sub> and  $\alpha$ -Ga<sub>2</sub>O<sub>3</sub> phases, respectively. We compared our results with bulk  $\beta$ -Ga<sub>2</sub>O<sub>3</sub>, and concluded that the phase-transition pressure and bulk modulus of nanocrystalline  $\beta$ -Ga<sub>2</sub>O<sub>3</sub> are higher than those of bulk counterpart.

© 2010 American Institute of Physics. [doi:10.1063/1.3296121]

### I. INTRODUCTION

Monoclinic gallium oxide ( $\beta$ -Ga<sub>2</sub>O<sub>3</sub>), a wide-band-gap semiconductor ( $E_g=4.9$  eV), exhibits unique conduction and luminescence properties and thus attracts much research interest due to numerous technological application.<sup>1–5</sup> Recently, considerable effort has been devoted to the study of nanostructured  $\beta$ -Ga<sub>2</sub>O<sub>3</sub> because of the potential for applications in nanodevices.<sup>6–10</sup> In ambient conditions, monoclinic  $\beta$ -Ga<sub>2</sub>O<sub>3</sub> is the thermodynamically stable form and there are other four metastable structures:  $\alpha$ -,  $\gamma$ -,  $\delta$ -, and  $\epsilon$ -Ga<sub>2</sub>O<sub>3</sub>.<sup>11</sup> Different forms have different physical properties. For example, the band gap of the  $\alpha$ -Ga<sub>2</sub>O<sub>3</sub> polymorph is 2.41 eV, much narrower than that of  $\beta$ -Ga<sub>2</sub>O<sub>3</sub>.<sup>12</sup> So it is important to clarify the relationship between different structures, which can be accessed by research on high-pressure phase transition. Especially for nanocrystal materials, investigation of the high-pressure behavior reveals the contribution of boundary in phase transition and provides additional insights into size-dependent changes in phase stability and mechanical properties.

The high-pressure behavior of  $\beta$ -Ga<sub>2</sub>O<sub>3</sub> had not received much attention until recently.<sup>13–21</sup> It is verified that  $\beta$ -Ga<sub>2</sub>O<sub>3</sub> undergoes a sluggish transition to  $\alpha$ -Ga<sub>2</sub>O<sub>3</sub> under high pressure. However, there is still a controversy on the value of the transition pressure. Machon *et al.*<sup>15</sup> indicated that  $\beta$ - to  $\alpha$ -Ga<sub>2</sub>O<sub>3</sub> phase transition occurred at 20–22 GPa, while Lipinska-Kalita *et al.*<sup>16</sup> found that transition began at 6.5–7 GPa at ambient temperature. Theoretical calculations based on density-functional theory gave the transition pressure of 2.6 GPa (Ref. 18) when the  $d$  electron of Ga was treated as core state, and of 6 GPa (Ref. 18) and 9.5 GPa (Ref. 19)

when the  $d$  electron of Ga as valence state. Lipinska-Kalita *et al.*<sup>16</sup> also reported that the transition pressure with and without transmitting medium were 6.5–7 and 3 GPa, respectively.

Research on high-pressure phase transition of nanocrystalline  $\beta$ -Ga<sub>2</sub>O<sub>3</sub> can only be found in the work of Lipinska-Kalita *et al.*<sup>21</sup> They reported the  $\beta$ - to  $\alpha$ -Ga<sub>2</sub>O<sub>3</sub> transition, beginning at 6 GPa, in nanocrystalline  $\beta$ -Ga<sub>2</sub>O<sub>3</sub> embedded in an amorphous silica matrix. However, they also mentioned that the silica glass matrix undergoes structural and density changes within this pressure range,<sup>22,23</sup> so that it is not yet known if the structural changes are intrinsic to nanocrystalline  $\beta$ -Ga<sub>2</sub>O<sub>3</sub>, or are promoted by anomalous densification among the silica matrix. These results encourage us to re-examine the high-pressure behavior of freestanding  $\beta$ -Ga<sub>2</sub>O<sub>3</sub> nanoparticles by angle-dispersive x-ray diffraction (XRD) technique.

### II. EXPERIMENTS

Monoclinic  $\beta$ -Ga<sub>2</sub>O<sub>3</sub> nanoparticles were synthesized as follows: 0.7 g GaCl<sub>3</sub>, 0.8 g NaOH and 4 ml PEG (Mw 400) were first dissolved in 10 ml ethanol, stirred with a magnetic stirrer. The precursory solution was stirred at 60 °C for 1 h to yield a transparent solution in an alumina crucible. The solution in the alumina crucible was then heated in a furnace at 900 °C for 3 h. The powder was white after annealing treatment. Finally, the white powder was washed using alcohol and centrifuged for three times, and then dried at 70 °C. The average crystallite size of Ga<sub>2</sub>O<sub>3</sub> nanoparticles was determined by XRD with a Cu  $K\alpha$  radiation and by transmission electron microscopy (TEM).

*In situ* angle-dispersive XRD measurements of nanocrystalline  $\beta$ -Ga<sub>2</sub>O<sub>3</sub> were performed at beam line BL-13A in High Energy Accelerator Research Organization (KEK).

<sup>a)</sup>Electronic mail: jjiangz@zju.edu.cn.

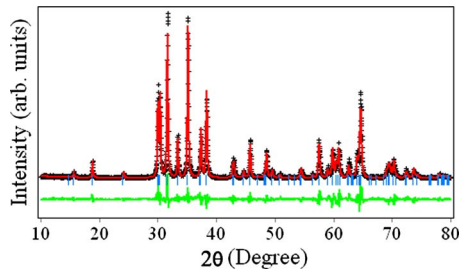


FIG. 1. (Color online) Full profile Rietveld refinement of diffraction pattern for nanocrystalline  $\beta$ - $\text{Ga}_2\text{O}_3$ . Asterisks, upper, and lower solid lines represent experimental, calculated, and difference pattern, respectively. Bars are marked at the positions of diffraction peaks.

Monochromatic x-ray ( $\lambda=0.42713 \text{ \AA}$ ) was collimated to  $50 \times 50 \mu\text{m}^2$  and irradiated at the center of the sample. Diffraction patterns were collected by image plate detector. The samples were compressed into a  $120 \mu\text{m}$  diameter hole drilled in a T301 stainless steel gasket of a Mao-Bell diamond-anvil cell. A mixture of methanol, ethanol, and water in the volume ratio of 16:3:1 was used as the pressure-transmitting medium. The pressures were determined by the ruby fluorescence method.<sup>24</sup>

### III. RESULTS AND DISCUSSION

Figure 1 shows the XRD pattern of as-prepared  $\text{Ga}_2\text{O}_3$  nanoparticles which was used to identify the structure and to estimate the mean grain size. A Rietveld full profile refinement<sup>25</sup> confirmed that all the peaks in the XRD pattern corresponded to the monoclinic  $\beta$ - $\text{Ga}_2\text{O}_3$  (space group  $C2/m$ ). No peaks of any other phases were detected. The refined  $\beta$ - $\text{Ga}_2\text{O}_3$  lattice parameters and cell volume were  $a=12.233(3) \text{ \AA}$ ,  $b=3.038(5) \text{ \AA}$ ,  $c=5.806(4) \text{ \AA}$ ,  $\beta=103.836(4)^\circ$ , and  $V=209.51(4) \text{ \AA}^3$ , in agreement with the values of bulk sample [ $a=12.233(10) \text{ \AA}$ ,  $b=3.038(3) \text{ \AA}$ ,  $c=5.807(5) \text{ \AA}$ ,  $\beta=103.821(7)^\circ$ , and  $V=209.56(4) \text{ \AA}^3$ ].<sup>16</sup> The average grain size of nanocrystalline  $\beta$ - $\text{Ga}_2\text{O}_3$  was estimated to be about 14 nm using the Scherrer formula, consistent with the average value of the grain size discerned in the TEM micrograph of Fig. 2(a). Each nanocrystal was roughly spherical and almost composed of a single-crystalline domain, as shown in Fig. 2.

Synchrotron XRD patterns of 14 nm  $\beta$ - $\text{Ga}_2\text{O}_3$  nanocrystal in the compression up to 64.9 GPa and the following decompression down to ambient pressure at room temperature were collected to analyze the pressure-induced phase transitions and to retrieve the isothermal bulk modulus. Some selected XRD patterns, which are characteristic of the

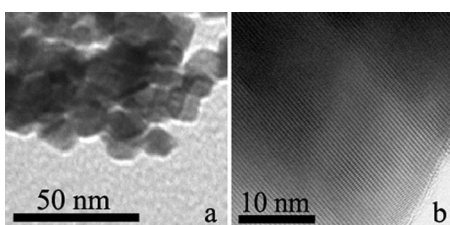


FIG. 2. Transmission electron microscopic patterns of nanocrystalline  $\beta$ - $\text{Ga}_2\text{O}_3$ : (a) low magnification image and (b) HRTEM image.

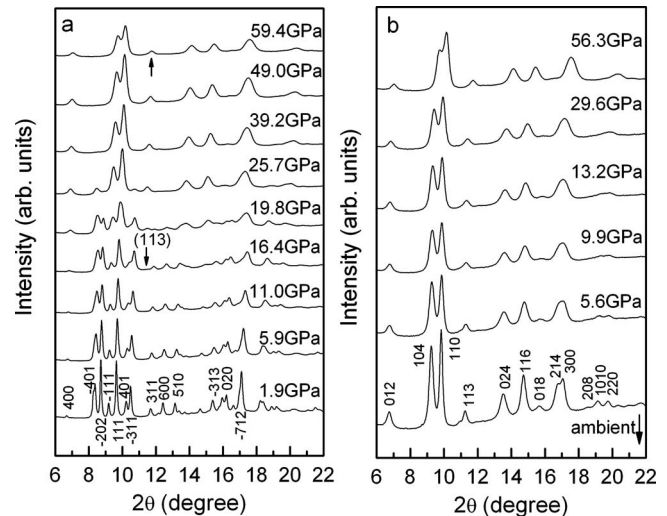


FIG. 3. Selected angle-dispersive synchrotron XRD patterns: (a) compression up to 64.9 GPa and (b) subsequent decompression. The appearance of the (113) peak for  $\alpha$ - $\text{Ga}_2\text{O}_3$  is arrowed.

whole evolution, are shown in Fig. 3. Diffraction line broadening at high pressure might be originated from nonhydrostaticity caused by solidification of pressure-transmitting medium at pressures above about 16 GPa. The diffraction patterns collected at low pressures correspond well to the monoclinic  $\beta$ - $\text{Ga}_2\text{O}_3$  phase. With increasing pressure, all diffraction peaks systematically shifted toward higher  $2\theta$  angles, and some peaks disappeared while new lines emerged. At 16.4 GPa, a new peak [arrowed in Fig. 3(a)] appeared, indicating occurrence of a phase transition. The phase transition proceeded slowly, and above 39.2 GPa, only peaks from the high-pressure phase remained to the highest pressure used in this study. The high-pressure diffraction patterns could be indexed within the  $R\bar{3}c$  space group expected for the rhombohedral  $\alpha$ - $\text{Ga}_2\text{O}_3$ , in accordance with former results.<sup>15,16,21</sup>

At the beginning of phase transition, the (104) and (110) peaks, two strong reflections of  $\alpha$ - $\text{Ga}_2\text{O}_3$ , were overlapped with the  $(\bar{1}11)$  and (111) peaks of the still dominating  $\beta$ - $\text{Ga}_2\text{O}_3$ , so the onset pressure of phase transition is imprecisely estimated only according to the appearance of the (113) peak. In order to confirm the pressure range of the  $\beta$ -to  $\alpha$ - $\text{Ga}_2\text{O}_3$  phase transition and to determine the lattice parameters, Rietveld refinements were performed on all diffraction patterns recorded during compression and subsequent decompression. The evolution of weight percent for  $\beta$ - $\text{Ga}_2\text{O}_3$  and  $\alpha$ - $\text{Ga}_2\text{O}_3$  with pressure is presented in Fig. 4. It is clearly shown that the weight percent of  $\beta$ - $\text{Ga}_2\text{O}_3$  keeps close to 100% below 13.6 GPa. For the pattern at 16.4 GPa, the Rietveld refinement confirmed that  $\beta$ - and  $\alpha$ - $\text{Ga}_2\text{O}_3$  phases coexisted with a ratio of 89.7:10.3 in wt %. It is obvious that the phase transition begins in the range of 13.6–16.4 GPa. The  $\beta$ - $\text{Ga}_2\text{O}_3$  was the dominating phase up to 19.8 GPa, and tiny  $\beta$ - $\text{Ga}_2\text{O}_3$  could still be detected at 36.8 GPa, indicating a sluggish transition in a wide pressure range of 13.6–39.2 GPa similar to the range of 6.5–40 GPa for bulk  $\text{Ga}_2\text{O}_3$ .<sup>16</sup>

All patterns collected from the decompression sequence only attribute to  $\alpha$ - $\text{Ga}_2\text{O}_3$ , and the gradual shift of diffraction

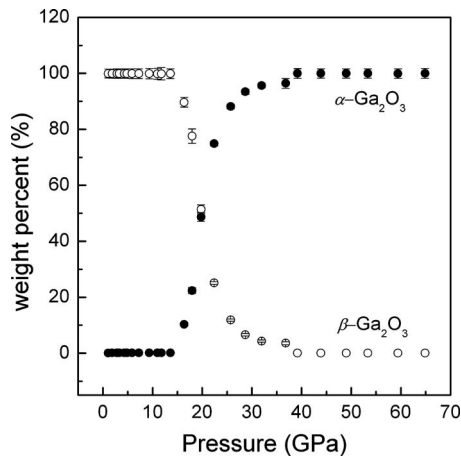


FIG. 4. The evolution of weight percent for  $\beta$ - $\text{Ga}_2\text{O}_3$  and  $\alpha$ - $\text{Ga}_2\text{O}_3$  with pressure during compression.

lines toward lower  $2\theta$  angles indicates a progressive relaxation of the  $\alpha$ - $\text{Ga}_2\text{O}_3$  structure, as shown in Fig. 3(b). That demonstrates the pressure-driven  $\beta$ - to  $\alpha$ - $\text{Ga}_2\text{O}_3$  phase transition is irreversible within the decompression time scale used here. Figure 5 illustrates Rietveld full profile refinements of the diffraction patterns of  $\alpha$ - $\text{Ga}_2\text{O}_3$  at 64.9 GPa and ambient pressure. The refinements yielded the following lattice parameters of  $\alpha$ - $\text{Ga}_2\text{O}_3$ :  $a=4.7807(9)$  Å,  $c=12.4743(29)$  Å at 64.9 GPa and  $a=4.9723(6)$  Å,  $c=13.4031(17)$  Å at ambient pressure, respectively. The ambient lattice parameters of  $\alpha$ - $\text{Ga}_2\text{O}_3$  correspond well with the results of Lipinska-Kalita *et al.*<sup>16</sup> [ $a=4.979(10)$  Å and  $c=13.432(28)$  Å].

Table I presents onset pressures of  $\beta$ - to  $\alpha$ - $\text{Ga}_2\text{O}_3$  phase

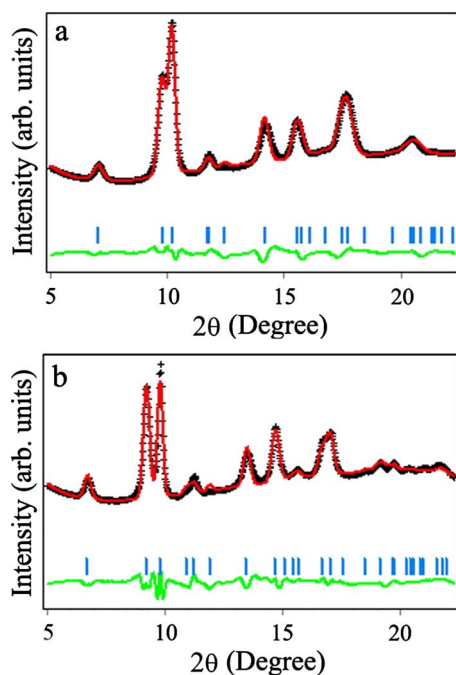


FIG. 5. (Color online) Full profile Rietveld refinements of diffraction patterns for  $\alpha$ - $\text{Ga}_2\text{O}_3$ : (a) at 64.9 GPa and (b) ambient pressure. Asterisks, upper, and lower solid lines represent experimental, calculated, and difference pattern, respectively. Bars are marked at the positions of diffraction peaks.

transition in our work and others. We found that the pressure-induced phase transition for freestanding  $\beta$ - $\text{Ga}_2\text{O}_3$  nanocrystal began within 13.6–16.4 GPa, higher than the previous result of 6 GPa for nanocrystalline  $\beta$ - $\text{Ga}_2\text{O}_3$  embedded in amorphous matrix.<sup>21</sup> It indicated that the host glass matrix could promote the occurrence of the  $\beta$ - to  $\alpha$ - $\text{Ga}_2\text{O}_3$  phase transition. The glass matrix would introduce the anisotropic stress on the nanocrystalline  $\beta$ - $\text{Ga}_2\text{O}_3$  embedded in it. The anisotropic stress is supposed to play an important role in the  $\beta$ - to  $\alpha$ - $\text{Ga}_2\text{O}_3$  phase transition. It was also proved by the Lipinska-Kalita *et al.*,<sup>16</sup> who found that the transition pressure was 3 GPa without transmitting medium, lower than 6.5–7 GPa with nitrogen as a pressure medium. In addition, the pressure-induced coordination change and densification of the host glass matrix could also influence the phase transition, as mentioned in Ref. 21.

As to onset pressure of bulk  $\beta$ - to  $\alpha$ - $\text{Ga}_2\text{O}_3$  transition, experimental data reported in recent years can be divided into two ranges of 3.3–7 and 20–22 GPa, respectively (Table I). Our result just exists between these two ranges. Thus it is difficult to judge the influence of grain size on the transition pressure. Jamieson<sup>26</sup> founded a relationship between transition pressure  $P_{tr}$  and energy band gap at ambient pressure  $E_g$  for semiconductors:  $P_{tr}\Delta V \propto E_g$ , where  $\Delta V$  is the volume deviation between two phases at  $P_{tr}$ . From transmission spectrum collected at ambient condition (Fig. 6), we obtained the band gap of 14 nm  $\beta$ - $\text{Ga}_2\text{O}_3$  as 5.9 eV, which is higher than 4.9 eV for bulk  $\beta$ - $\text{Ga}_2\text{O}_3$ . By substituting  $E_g$  and  $\Delta V$  of bulk and nanocrystalline  $\beta$ - $\text{Ga}_2\text{O}_3$  into Jamieson's function, it is deduced that the transition pressure  $P_{tr}$  for the nanocrystalline sample is higher than that for the bulk one. Based on this analysis as well as theoretical calculation results of 2.6–9 GPa for the phase transition pressure of  $\beta$ - to  $\alpha$ - $\text{Ga}_2\text{O}_3$  (Table I), it is more reasonable to consider the onset pressure of phase transition for bulk sample in the range of 3.3–7 GPa. Therefore, we can conclude that the phase transition pressure of freestanding nanocrystalline  $\beta$ - $\text{Ga}_2\text{O}_3$  is higher than that of bulk material, consistent with the results of other nanocrystalline materials.<sup>27–30</sup>

The evolution of the lattice parameters with pressure for  $\beta$ - $\text{Ga}_2\text{O}_3$  and  $\alpha$ - $\text{Ga}_2\text{O}_3$  is presented in Fig. 7, and the linear compressibilities are summarized in Table II. The lattice compression of both gallium oxide phases is anisotropic, with the  $a$  and  $b$  axes more compressible than the  $c$  axis in the monoclinic  $\beta$ - $\text{Ga}_2\text{O}_3$  structure, and with the  $c$  axis more compressible than the  $a$  axis in the rhombohedral  $\alpha$ - $\text{Ga}_2\text{O}_3$  structure. The monoclinic angle decreased with increasing pressure, in agreement with the tendency in Ref. 15. The compressibility values along the  $b$  and  $c$  axes of  $\beta$ - $\text{Ga}_2\text{O}_3$  in our study are comparable with those obtained previously for bulk  $\beta$ - $\text{Ga}_2\text{O}_3$  (Ref. 15) and for nanocrystalline samples embedded in amorphous silica.<sup>21</sup> However, the  $a$  axis compression is only comparable with that of bulk  $\beta$ - $\text{Ga}_2\text{O}_3$ ,<sup>15</sup> while twice as large as that of nanocrystalline samples embedded in amorphous silica. Such difference in compressibility along the  $a$  axis might be explained by the possibility that host glass matrix surrounding the  $\beta$ - $\text{Ga}_2\text{O}_3$  nanocrystal could accommodate and relax the strains. The ratio of  $c/a$  for the

TABLE I. Comparison of bulk modulus  $B_0$  and unit-cell volume  $V_0$  of  $\beta$ -Ga<sub>2</sub>O<sub>3</sub> and  $\alpha$ -Ga<sub>2</sub>O<sub>3</sub> at ambient conditions, and onset pressure of  $\beta$ -to  $\alpha$ -Ga<sub>2</sub>O<sub>3</sub> transition in our study with those reported.

Sample	Beginning of phase transition	$\beta$ -Ga <sub>2</sub> O <sub>3</sub>			$\alpha$ -Ga <sub>2</sub> O <sub>3</sub>			Method
		$B_0$ (GPa)	$B'_0$	$V_0$ (Å <sup>3</sup> )	$B_0$ (GPa)	$B'_0$	$V_0$ (Å <sup>3</sup> )	
14 nm <sup>a</sup>	13.6–16.4 GPa	193(6)	9.8(9)	207.0(8)	354(22)	3.0(4)	287.0(7)	ADX
		228(9)	4	207.0(8)	333(19)	4	287.0(7)	
14.8 nm <sup>b</sup>	6 GPa	191(5)	8.3(9)	209.5(3)				EDX
Bulk <sup>c</sup>	6.5–7 GPa	199(6)	3.1(4)	209.1(2)	220(9)	5.9(6)	288(1)	ADX
		184(3)	4	209.4(2)	252(14)	4	288(1.5)	
Bulk <sup>d</sup>	7.6 GPa, 1500 K	255(16)	7.63(90)	209.9(4)	261(20)	7.93(71)	288.8(1)	ADX
		134(12)	4	209.24	223(2)	4	288.96(24)	
		142	4.1	204.56	243	4.0	283.44	DFT
Bulk <sup>e</sup>	20–22 GPa	202(7)	2.4(6)					ADX
Bulk <sup>f</sup>	9.5	174	3.79		210	4.95		DFT
Bulk <sup>g</sup>	2.6 or 6 GPa							DFT

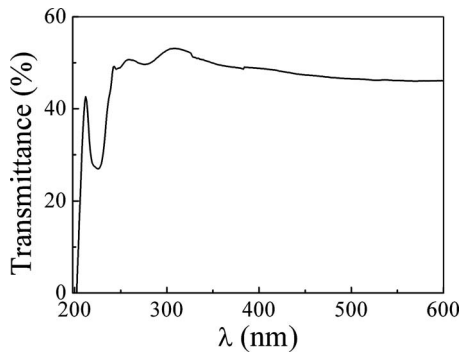
<sup>a</sup>This study.<sup>b</sup>Reference 21.<sup>c</sup>Reference 16.<sup>d</sup>Reference 17.<sup>e</sup>Reference 15.<sup>f</sup>Reference 19.<sup>g</sup>Reference 18.

$\alpha$ -Ga<sub>2</sub>O<sub>3</sub> linearly decreased during compression and then increased from 2.609 at 64.9 GPa to 2.696 at ambient pressure during decompression.

The  $V/V_0$  relations as a function of pressure for nanocrystalline  $\beta$ -Ga<sub>2</sub>O<sub>3</sub> and  $\alpha$ -Ga<sub>2</sub>O<sub>3</sub> during compression are shown in Fig. 8. At 16.4 GPa, the volume collapse across the phase transition was about 6.5%. The  $P$ - $V$  data were fitted using a third-order Birch–Murnaghan equation of state

$$P = 1.5B_0[(V/V_0)^{-7/3} - (V/V_0)^{-5/3}] \times \{1 + 0.75(B'_0 - 4) \times [(V/V_0)^{-2/3} - 1]\},$$

where  $V_0$  is the volume at ambient pressure,  $B_0$  is the bulk modulus at ambient pressure, and  $B'_0$  is the pressure derivative at ambient pressure. The fitting parameters  $B_0$  and  $B'_0$  are summarized in Table I, where reported data are also presented. Since the value of  $B'_0$  differs largely between the two phases, we fitted again the compression data by fixing  $B'_0 = 4$  to give a better idea of the relative compressibility between  $\beta$ -Ga<sub>2</sub>O<sub>3</sub> and  $\alpha$ -Ga<sub>2</sub>O<sub>3</sub> phases. It should be pointed out that the data of minor phase while two phases coexist,  $\alpha$ -Ga<sub>2</sub>O<sub>3</sub> phase at low pressure and  $\beta$ -Ga<sub>2</sub>O<sub>3</sub> phase at high pressure, were not fitted because of their large uncertainty.

FIG. 6. The optical transmission spectrum of 14 nm  $\beta$ -Ga<sub>2</sub>O<sub>3</sub> at ambient condition.

As shown in Table I, the bulk modulus of 14 nm  $\beta$ -Ga<sub>2</sub>O<sub>3</sub> in our work is close to that of nanocrystalline sample embedded in glass matrix and slightly higher than

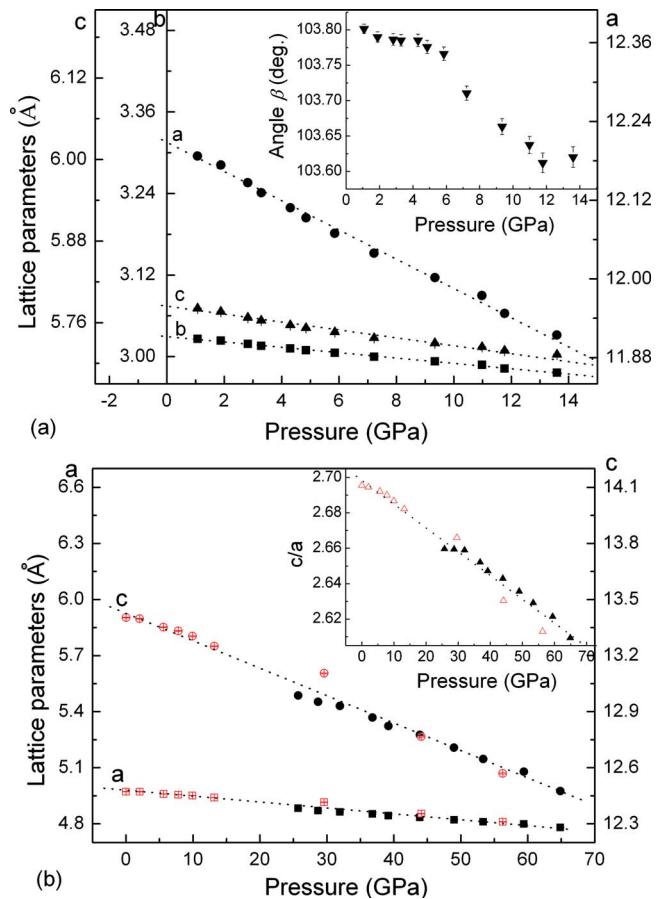
FIG. 7. (Color online) Pressure evolution of lattice parameters: (a) of the  $\beta$ -Ga<sub>2</sub>O<sub>3</sub>, and (b) of the  $\alpha$ -Ga<sub>2</sub>O<sub>3</sub>. Solid and open symbols refer to the compression and decompression data, respectively. The differential (in angstrom) of the vertical scales of each graph is the same, in order to facilitate comparison between the evolutions of lattice parameters. Dot lines are drawn as a guide for the eyes.

TABLE II. Comparison of linear compressibilities of  $\beta$ -Ga<sub>2</sub>O<sub>3</sub> and  $\alpha$ -Ga<sub>2</sub>O<sub>3</sub> in our study with data reported.

Linear compressibility	14 nm <sup>a</sup>		14.8 nm <sup>b</sup>	Bulk <sup>c</sup>
	$\alpha$ -Ga <sub>2</sub> O <sub>3</sub>	$\beta$ -Ga <sub>2</sub> O <sub>3</sub>	$\beta$ -Ga <sub>2</sub> O <sub>3</sub>	$\beta$ -Ga <sub>2</sub> O <sub>3</sub>
$\beta_a$ (GPa <sup>-1</sup> )	$6.21(5) \times 10^{-4}$	$1.78(7) \times 10^{-3}$	$8.2 \times 10^{-4}$	$1.99(9) \times 10^{-3}$
$\beta_b$ (GPa <sup>-1</sup> )		$1.30(6) \times 10^{-3}$	$1.97 \times 10^{-3}$	$1.45(2) \times 10^{-3}$
$\beta_c$ (GPa <sup>-1</sup> )	$1.10(3) \times 10^{-3}$	$9.34(9) \times 10^{-4}$	$8.8 \times 10^{-4}$	$8.8(4) \times 10^{-4}$

<sup>a</sup>This study.<sup>b</sup>Reference 21.<sup>c</sup>Reference 15.

that of bulk  $\beta$ -Ga<sub>2</sub>O<sub>3</sub>, while bulk modulus of  $\alpha$ -Ga<sub>2</sub>O<sub>3</sub> in our work is much higher than that of the bulk material which might be connected with the high surface energy of  $\alpha$ -Ga<sub>2</sub>O<sub>3</sub>. Further investigation is required to get a better understanding of this elevation.

#### IV. CONCLUSIONS

The high-pressure behavior of 14 nm  $\beta$ -Ga<sub>2</sub>O<sub>3</sub> particles was investigated using angle-dispersive synchrotron XRD up to 64.9 GPa. It was found that the onset transition pressure of  $\beta$ - to  $\alpha$ -Ga<sub>2</sub>O<sub>3</sub> was within 13.6–16.4 GPa, and phase transition was sluggish and irreversible with  $\alpha$ -Ga<sub>2</sub>O<sub>3</sub>, remaining after pressure release. Based on the first principles calculations reported and the relationship between the transition pressure and energy gap, we conclude that the transition pressure of nanocrystalline  $\beta$ -Ga<sub>2</sub>O<sub>3</sub> is higher than that of bulk counterpart. According to the hydrostatic compression data, the bulk modulus at a fixed  $B'_0=4$  of nanocrystalline  $\beta$ -Ga<sub>2</sub>O<sub>3</sub> and  $\alpha$ -Ga<sub>2</sub>O<sub>3</sub> was estimated at 228(9) GPa and 333(19) GPa, both higher than the bulk materials, respectively.

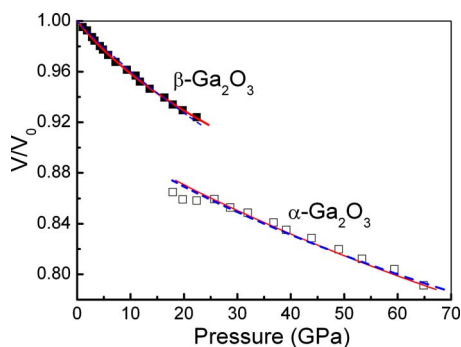


FIG. 8. (Color online) The evolution of  $V/V_0$  for  $\beta$ -Ga<sub>2</sub>O<sub>3</sub> and  $\alpha$ -Ga<sub>2</sub>O<sub>3</sub> with pressure. Solid lines and dashed lines are the Birch–Murnaghan equation of state fits to experimental data with unfixed  $B'_0$ , and with fixed  $B'_0=4$ , respectively.

#### ACKNOWLEDGMENTS

The authors would like to thank the KEK, Japan, for the assistance during the high-pressure x-ray diffraction measurements. Financial support from the National Natural Science Foundation of China (Grant Nos. 50701038, 60776014, 60876002, 10804096, 50920105101, and 10979002), Zhejiang University–Helmholtz cooperation fund, the Ministry of Education of China (Program for Changjiang Scholars and the Research Fund for the Doctoral Program of Higher Education), the Department of Science and Technology of Zhejiang Province, and Zhejiang University is gratefully acknowledged.

- <sup>1</sup>L. Binet and D. Gourier, *J. Phys. Chem. Solids* **59**, 1241 (1998).
- <sup>2</sup>M. Ogita, N. Saika, Y. Nakanishi, and Y. Hatanaka, *Appl. Surf. Sci.* **142**, 188 (1999).
- <sup>3</sup>M. Passlack, E. F. Schubert, W. S. Hobson, M. Hong, N. Moriya, S. N. G. Chu, K. Konstadinidis, J. P. Mannaerts, M. L. Schnoes, and G. J. Zydzik, *J. Appl. Phys.* **77**, 686 (1995).
- <sup>4</sup>T. Miyata, T. Nakatani, and T. Minami, *Thin Solid Films* **373**, 145 (2000).
- <sup>5</sup>Z. Li, C. de Groot, and J. H. Moodera, *Appl. Phys. Lett.* **77**, 3630 (2000).
- <sup>6</sup>Y. C. Choi, W. S. Kim, Y. S. Park, S. M. Lee, D. J. Bae, Y. H. Lee, G. S. Park, W. B. Choi, N. S. Lee, and J. M. Kim, *Adv. Mater.* **12**, 746 (2000).
- <sup>7</sup>R. Rao, A. M. Rao, B. Xu, J. Dong, S. Sharma, and M. K. Sunkara, *J. Appl. Phys.* **98**, 094312 (2005).
- <sup>8</sup>C. H. Liang, G. W. Meng, G. Z. Wang, Y. W. Wang, L. D. Zhang, and S. Y. Zhang, *Appl. Phys. Lett.* **78**, 3202 (2001).
- <sup>9</sup>S. Sharma and M. K. Sunkara, *J. Am. Chem. Soc.* **124**, 12288 (2002).
- <sup>10</sup>J. S. Kim, H. E. Kim, H. L. Park, and G. C. Kim, *Solid State Commun.* **132**, 459 (2004).
- <sup>11</sup>R. Roy, V. G. Hill, and E. F. Osborn, *J. Am. Chem. Soc.* **74**, 719 (1952).
- <sup>12</sup>H. G. Kim and W. T. Kim, *J. Appl. Phys.* **62**, 2000 (1987).
- <sup>13</sup>T. P. Beales, C. H. L. Goodman, and K. Scarrott, *Solid State Commun.* **73**, 1 (1990).
- <sup>14</sup>B. Tu, Q. Cui, P. Xu, X. Wang, W. Gao, C. Wang, J. Liu, and G. Zou, *J. Phys.: Condens. Matter* **14**, 10627 (2002).
- <sup>15</sup>D. Machon, P. F. McMillan, B. Xu, and J. Dong, *Phys. Rev. B* **73**, 094125 (2006).
- <sup>16</sup>K. E. Lipinska-Kalita, P. E. Kalita, O. A. Hemmers, and T. Hartmann, *Phys. Rev. B* **77**, 094123 (2008).
- <sup>17</sup>H. Yusa, T. Tsuchiya, N. Sata, and Y. Ohishi, *Phys. Rev. B* **77**, 064107 (2008).
- <sup>18</sup>P. Kroll, *Phys. Rev. B* **72**, 144407 (2005).
- <sup>19</sup>H. He, R. Orlando, M. A. Blanco, R. Pandey, E. Amzallag, I. Baraille, and M. Rerat, *Phys. Rev. B* **74**, 195123 (2006).
- <sup>20</sup>R. Caracas and R. E. Cohen, *Phys. Rev. B* **76**, 184101 (2007).
- <sup>21</sup>K. E. Lipinska-Kalita, B. Chen, M. B. Kruger, Y. Ohki, J. Murowchick, and E. P. Gogol, *Phys. Rev. B* **68**, 035209 (2003).
- <sup>22</sup>M. Grimsditch, *Phys. Rev. Lett.* **52**, 2379 (1984).
- <sup>23</sup>C. Meade, R. J. Hemley, and H. K. Mao, *Phys. Rev. Lett.* **69**, 1387 (1992).
- <sup>24</sup>H. K. Mao, P. M. Bell, J. W. Shaner, and D. J. Steinberg, *J. Appl. Phys.* **49**, 3276 (1978).
- <sup>25</sup>H. M. Rietveld, *J. Appl. Crystallogr.* **2**, 65 (1969).
- <sup>26</sup>J. C. Jamieson, *Science* **139**, 845 (1963).
- <sup>27</sup>S. H. Tolbert and A. P. Alivisatos, *Science* **265**, 373 (1994).
- <sup>28</sup>S. B. Qadri, J. Yang, B. R. Ratna, E. F. Skelton, and J. Z. Hu, *Appl. Phys. Lett.* **69**, 2205 (1996).
- <sup>29</sup>J. Z. Jiang, L. Gerward, D. Frost, R. Secco, J. Peyronneau, and J. S. Olsen, *J. Appl. Phys.* **86**, 6608 (1999).
- <sup>30</sup>Y. He, J. F. Liu, W. Chen, Y. Wang, H. Wang, Y. W. Zeng, G. Q. Zhang, L. N. Wang, J. Liu, T. D. Hu, H. Hahn, H. Gleiter, and J. Z. Jiang, *Phys. Rev. B* **72**, 212102 (2005).